Polymer Journal

REGULAR ARTICLE

Synthesis and Properties of New Small Band Gap Conjugated Polymers: Methine Bridged Poly(3,4-ethylenedioxypyrrole)

By Jung-Hsun TSAI,[1] *Wei-Ren TU,*[2] *Cheng-Liang LIU,*[1] *Wen-Chung WU,*[2] *and Wen-Chang CHEN*[1,2,*]

Synthesis and electronic properties of new small band gap conjugated polymers, methine-bridged poly(3,4-ethylenedioxypyrrole) (**PEDOP**) are reported. Density functional theory (B3LYP with 6-31G basis) are used to obtain the optimized ground-state geometries and electronic structures of **PEDOP** and poly[(3,4-ethylenedioxypyrrole-2,5-diyl) methine] (**PEDOP-M**). Theoretical bond length alternation of **PEDOP** is reduced by incorporating the methine bridge and leads to the band gap reduction from 2.44 to 0.68 eV. The small band gap characteristic of **PEDOP-M** is further verified by preparing two conjugated polymers, poly[(2,5-*n*-benzyl-3,4-ethylenedioxypyrrolediyl)-benzylidene-(2,5-*n*-benzyl-3,4-ethylenedioxypyrrole-quinodimethanediyl)] (**PbEDOP-b**) and poly[(2,5-*n*-benzyl-3,4-ethylenedioxypyrrolediyl)-(*p*-nitrobenzylidene)-(2,5-*n*-benzyl-3,4-ethylenedioxypyrrole-quinodimethanediyl)] (**PbEDOP-nb**). The optical band gap of **PbEDOP-b** and **PbEDOP-nb** are 1.77 and 1.45 eV, respectively, while the electrochemical band gap of the former is 1.59 eV. Although the bulky side groups of these two polymers result in a larger band gap than that of **PEDOT-M**, it indicates the small band gaps of such polymers. The nitrobenzene group could extend the π-conjugation and lead to the smaller band gap of **PbEDOP-nb** than that of **PbEDOP-b**. The present study suggests that methine-bridged poly(3,4-ethylenedioxypyrrole) is a class of small band gap polymers.

KEY WORDS: Methine Bridged Polymers / Small Band Gap Polymers / Poly(3,4-ethylenedioxypyrrole) / Density Functional Theory /

Small band gap (E_g) conjugated polymers have been extensively studied[1–4] due to their potential applications in organic optoelectronic devices,[1–12] such as photovoltaic cells,[5,6] thin film transistors,[7] light emitting diodes,[8–10] electrochromic devices,[11] and supercapacitors.[12] The band gap of conjugated polymers can be manipulated through the molecular structures, such as bond length alternation (BLA), planarity, aromaticity, or donor/acceptor characteristics.[1–3] Representative small band gap polymers include poly(isothianaphthene) (PITN),[13,14] poly(thiophene methine) (PTMs),[15–18] polysquaraines,[3] poly(thiopyrazine),[19,20] poly(cyclopentadithiophene),[21] poly(thieno[3,4,b]thiophene),[22] and ladder polymers.[1–3]

Conjugated polymers with alternating aromatic and quinoid isomers were shown to have intrinsic small band gaps, including poly(thiophene methine) (PTM),[15–18] poly(isothianaphthene methine),[23,24] poly(pyrrole methine),[25] and poly[(3,4-ethylenedioxythiophene-2,5-diyl) methine].[26–28] In particular, the methine bridged conjugated polymers with the thiophene backbone exhibited relatively smaller band gap less than 1.0 eV. Recently, poly(3,4-dioxypyrrole) (**PXDOP**) has been widely studied since it exhibits unique properties of high conductivity, multicolor electrochromism, and rapid redox switching.[29–32] Although the oxidation potentials of **PXDOPs** are very low (<0.05 V versus SCE), they exhibit middle to high band gaps of 2.0–3.4 eV.[30] Besides, methine bridged poly(3,4-dioxypyrrole) have not been synthesized and characterized yet. Therefore, it would be worthwhile to explore the synthesis and properties of small band gap poly(3,4-ethylenedioxypyrrole) (**PEDOP**, **1** in Scheme 1) derivatives through the methine-bridged approach, such as **PEDOP** (**PEDOP-M**, **2** in Scheme 1).

In this study, we report the synthesis and electronic properties of the methine bridged **PEDOP**. It is the first report on synthesis of such polymer to the best of our knowledge. Theoretical calculations based on density functional theory (DFT) were performed to obtain the ground-state geometries and electronic structures of **PEDOP** and **PEDOP-M**. Two methine-bridged **PbEDOP** derivatives, **PbEDOP-b** and **PbEDOP-nb** (**3a** and **3b**, in Scheme 1), were synthesized *via* the acid-catalyzed polymerization of *n*-benzyl-3,4-ethylenedioxypyrrole (**bEDOP**) with benzaldehyde and 4-nitrobenzaldehyde, respectively. The bulky side groups at the bridge carbon of polymers **3** were introduced to provide enhanced solubility as compared with **PEDOP-M**. For the synthesis of small band gap conjugated polymers from acid-catalyzed polymerization, the mechanism of forming aromatic and quionid structure in the polymer structure was due to the dehydrogenation reaction from the methylene bridged polymers, poly(thiophene methine)[15] or poly(3,4-ethylenedioxythiophene methine) (**PEDOT-M**).[28] The theoretical electronic properties of the non-substituted **PEDOT-M** were shown to be consistent with the experimental results from the bulky side

[1]Department of Chemical Engineering, National Taiwan University, Taipei, Taiwan 106
[2]Institute of Polymer Science and Engineering, National Taiwan University, Taipei, Taiwan 106
*To whom correspondence should be addressed (Tel: +886-2-23628398, Fax: +886-2-23623040, E-mail: chenwc@ntu.edu.tw).

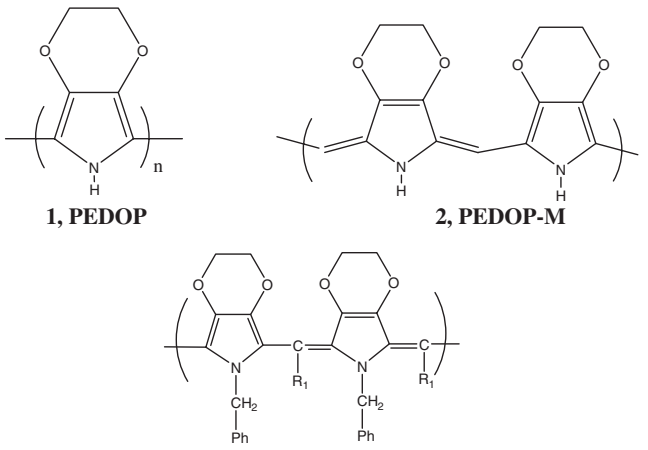

Scheme 1.

group-substituted analogs. Hence, the acid-catalyzed polymerization of *n*-benzyl-3,4-ethylenedioxypyrrole (**bEDOP**) with benzaldehyde and 4-nitrobenzaldehyde would lead to the proposed polymer structure with alternating aromatic and quionid structure. Also, the theoretical calculation on the electronic properties of **PEDOP-M** could be used to compare with the experimental results from **PbEDOP-b** and **PbEDOP-nb**. The polymer structures, thermal, optical and electrochemical properties of polymers **3** were characterized. The experimental electronic properties of the prepared methine-bridged **PbEDOP** derivatives were compared with those from the theoretical results to justify the small band gap characteristics.

Theoretical Methodology on the Electronic Structure

All of the calculations were performed on Gaussain03[33] by using density functional theory (DFT): Becke's three-parameter hybrid functional[34] combined with Lee, Yang, and Parr's correlation functional[35,36] (B3LYP) was used with 6-31G basis set. The geometries and electronic properties were calculated by assuming all the polymers to be isolated, infinite, one dimensional (linear) polymers. The starting unit cell geometries were taken from the central part of corresponding oligomers, and then fully optimized to the equilibrium geometries inside a given lattice length on the constraints of periodic boundary conditions by assuming that the unit cell is repeated identically an infinite number of times along the translation vector. Both the lattice parameter and molecular structures were varied to locate the lowest energy position in the unit cell.

EXPERIMENTAL

Materials

Benzyl-3,4-ethylenedioxypyrrole-2,5-dicarboxylate (95%, Aldrich), triethanolamine (99%, Riedel-deHaën), benzaldehyde (>98%, Acros), 4-nitrobenzaldehyde (99%, Acros), sulfuric acid (Baker, 96%), hydrochloric acid and solvents were purchased from Aldrich or Acros without further purification.

Synthesis

The synthetic routes of monomers and corresponding polymers are shown in Scheme 2. 6-benzyl-3,6-dihydro-2H-[1,4]dioxino[2,3-c]pyrrole-5,7-dicarboxylic acid (**1**) and 6-benzyl-3,6-dihydro-2H-[1,4]dioxino[2,3-c]pyrrole (**bEDOP**, **2**), were synthesized according to the literature.[32] The general procedure of synthesizing methine-bridged polymers of **PbEDOP-b** and **PbEDOP-nb** were through acid-catalyzed polymerization reported previously by one of us.[15,16]

Poly[(2,5-*n*-benzyl-3,4-ethylenedioxypyrrolediyl)benzylidene-(2,5-*n*-benzyl-3,4-ethylenedioxypyrrole-quinodimethanediyl)] (*PbEDOP-b*). The polymerization mixture was *n*-benzyl-3,4-ethylenedioxypyrrole (300 mg, 1.39 mmol), benzaldehyde (174.34 mg, 1.61 mmol), 4 mL of *p*-dioxane, and 47 mg (0.46 mmol) of 98% sulfuric acid. The reaction temperature was kept at 65 °C for 24 h. A dark purple reaction solution was precipitated into 300 mL of stirring methanol, recovered, recrystallized from THF/hexane, and dried in a vacuum oven at 40 °C for 12 h. The yield was 60%. ^{1}H NMR (DMSO-d_6): $\delta = 3.40$–4.38 (8H, 4(–CH_2)), 4.52–5.30 (4H, 2(–CH_2)), 6.00–7.65 (20H, phenyl rings). Molecular weight: weight-average molecular weight (M_w) = 4930, polydispersity index (PDI) = 1.62. Anal. Calcd. for $(C_{40}H_{33}N_2O_4)_n$: C, 79.45; H, 5.33; N, 4.63. Found: C, 77.40; H, 5.71; N, 4.48. FT-IR (film on KBr, cm^{-1}): 3058, 3025, 2940, 2859, 1601, 1491, 1452.

Poly[(2,5-*n*-benzyl-3,4-ethylenedioxypyrrolediyl)(*p*-nitrobenzylidene)(2,5-*n*-benzyl-3,4-ethylenedioxypyrrolequinodimethanediyl)] (*PbEDOP-nb*). The polymerization mixture was *n*-benzyl-3,4-ethylenedioxypyrrole (400 mg, 1.85 mmol), 4-nitrobenzaldehyde (325.66 mg, 2.15 mmol), 5 mL of *p*-dioxane, and 63 mg (0.62 mmol) of 98% sulfuric acid. The reaction temperature was kept at 60 °C for 24 h. A dark purple reaction solution was precipitated into 400 mL of stirring methanol, recovered, recrystallized from THF/hexane, and dried in a vacuum oven at 40 °C for 12 h. The yield was 70%. ^{1}H NMR (DMSO-d_6): $\delta = 3.40$–4.40 (8H, 4(–CH_2)), 4.40–5.31 (4H, 2(–CH_2)), 6.02–8.45 (18H, phenyl rings). Anal. Calcd. for $(C_{40}H_{30}N_4O_8)_n$: C, 69.39; H, 4.88; N, 7.83. Found: C, 67.56; H, 4.90; N, 7.57. FT-IR (film on KBr, cm^{-1}): 3062, 3030, 2973, 2927, 2869, 1585, 1573, 1516, 1452, 1343. Molecular weight: $M_w = 5160$, PDI = 1.30.

Characterization

^{1}H nuclear magnetic resonance (NMR) data was obtained by a Bruker AV 300 MHz spectrometer. FT-IR spectrum of the prepared polymer on KBr pellet was obtained using a Jasco Model FT-IR 410 spectrophotometer at room temperature. The sample was scanned 32 times with resolution 4 cm^{-1}. Gel permeation chromatographic analysis was performed on a Lab Alliance RI2000 instrument (two column, MIXED-C and D from Polymer Laboratories) connected with one refractive index detector from Schambeck SFD Gmbh. All GPC analyses were performed on polymer/THF solution at a flow rate of 1 mL/min at 40 °C and calibrated with polystyrene standards.

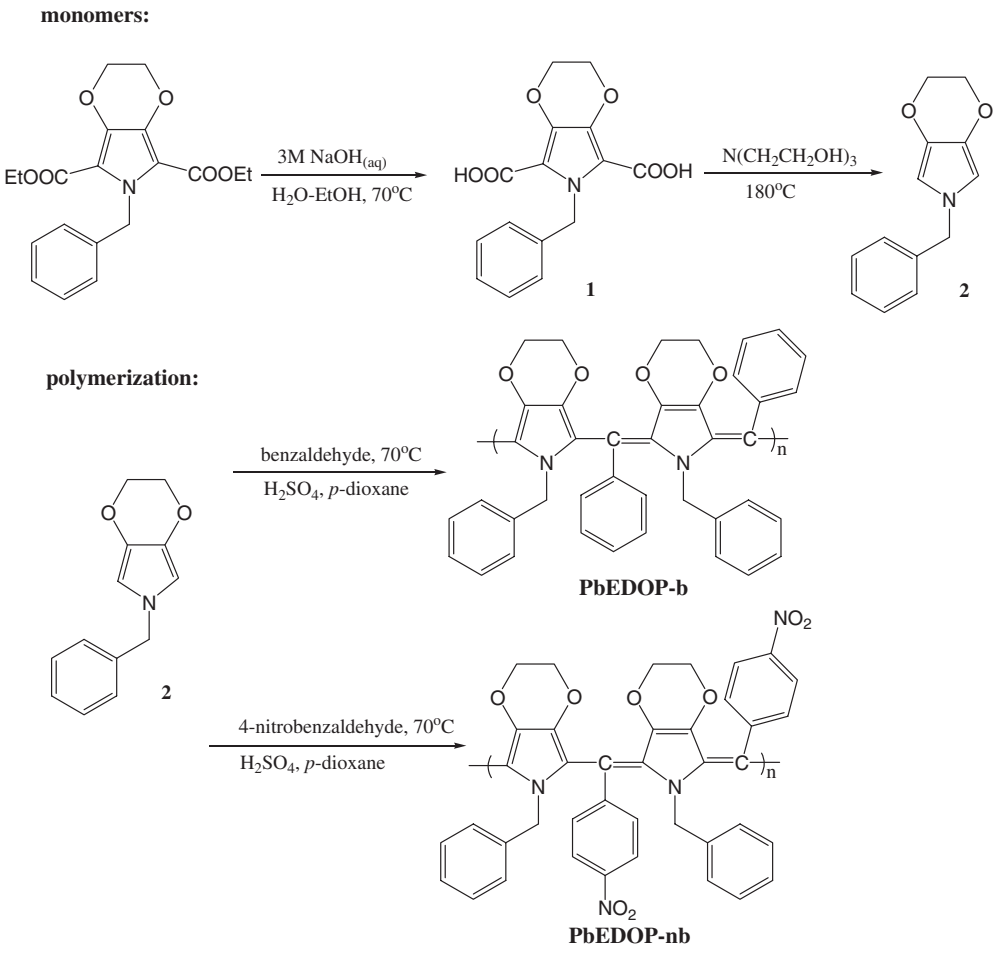

Scheme 2.

Thermogravimetric analysis (TGA) and differential scanning calorimetry (DSC) measurements were performed under a nitrogen atmosphere at a heating rate of 20 and 10 °C/min using a TA instrument TGA-951 and DSC-910S, respectively. UV–visible absorption spectra were recorded on a Jasco model UV/VIS/NIR V-570 spectrometer. For the solution spectra, polymers were dissolved in THF (*ca.* 10^{-6} M) and then put in a quartz cell for measurement. For the thin film spectra, polymers were first dissolved in THF (1 wt %) and then spin-coated on glass substrate at 1000 rpm for 30 s. Then, the thin film samples were dried at 60 °C under vacuum for measurement.

The electrochemical properties of the polymer films were investigated on a Princeton Applied Research Model 273A Potentiostat/Galvanostat with a 0.1 M acetonitrile (99.5+%, Tedia) solution containing tetrabutylammonium tetrafluoroborate ($TBABF_4$) (Fluka, >99.9%) as the electrolyte. Platinum wire and rod-tip electrodes were used as counter and working electrodes respectively. Silver/silver ion (Ag in 0.1 M $AgNO_3$ (Acros, 99.8%) in the supporting electrolyte solutions) was used as a reference electrode. A 3 wt % solution of a polymer in THF or DMSO was used to prepare the polymer film on the Pt rod-tip electrode. Then, the cyclic voltammetry of films was performed on a three-electrode cell. The reference electrode was calibrated through by the cyclic voltammetry of ferrocene without any polymer added into the solution. The cyclic voltammograms were obtained at a voltage scan rate of 40 mV/s. The potential values obtained versus Fc^+/Fc standard were converted to the saturated calomel electrode (SCE) scale by adding a constant voltage to them. The energy parameters EA and IP were estimated from the measured redox potentials on the basis of the prior work on conjugated polymers which has shown that: $IP = (E_{ox} + 4.4)$ and $EA = (E_{red} + 4.4)$, where the onset potentials are in volts (*vs.* SCE) and IP and EA are in electron volts. The 4.4 eV constant in the relation among IP, EA, and redox potentials is the SCE energy level versus vacuum. The electronic structure parameters, HOMO and LUMO, were estimated with the relation of HOMO = −IP and LUMO = −EA by assuming no configuration interactions.

RESULT AND DISCUSSION

Geometric and Electronic Structures of Studied Polymers

Theoretical analysis on the geometries and electronic structures of **PEDOP** and **PEDOP-M** was performed to investigate the effect of methine-bridged backbone on the electronic properties. Figure 1 shows the optimized unit cell

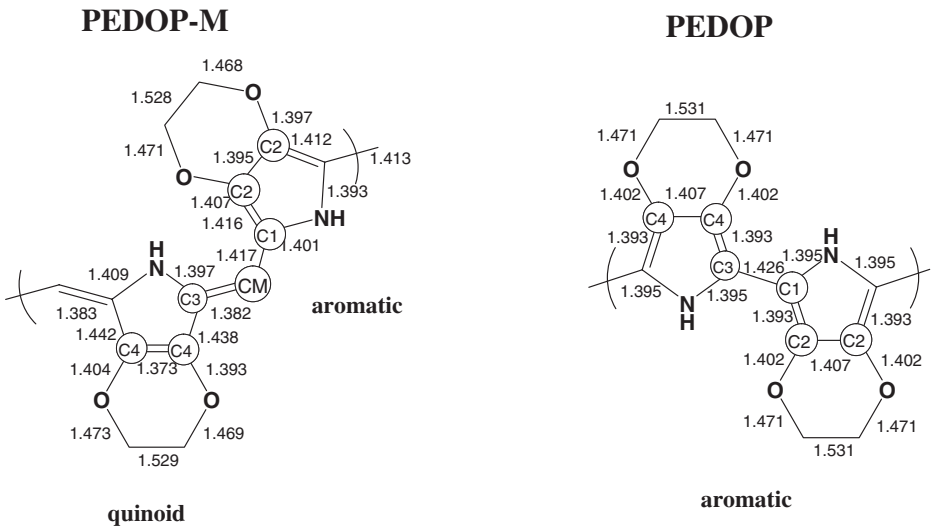

Figure 1. The optimized unit cell geometries of **PEDOP-M** and **PEDOP**.

Table I. Geometric and electronic parameters of **PEDOP-M** and **PEDOP**

	bond lengths (Å)[a]				electronic parameters[b]		
	$R_{(C1\text{-}CM)}/R_{(C3\text{-}CM)}$	$R_{(C1\text{-}C2)}/R_{(C2\text{-}C2)}$	$R_{(C3\text{-}C4)}/R_{(C4\text{-}C4)}$	BLA	IP (eV)	EA (eV)	E_g (eV)
PEDOP-M	1.417/1.382	1.416/1.395	1.438/1.373	0.028	2.54	1.86	0.68
PEDOP	—	1.393/1.407	1.393/1.407	0.033	2.98	0.54	2.44

[a]The numbering of carbon atoms is shown in Figure 1. [b]IP/EA estimated as below: IP = −HOMO, EA = −LUMO.

geometry of **PEDOP-M** and **PEDOP**, and the corresponding geometric and electronic parameters are listed in Table I. In general, a smaller bond length alternation (BLA, of adjacent C-C and C=C bonds on the backbone) provides a better π-delocalization through the polymer backbone and usually leads to a smaller band gap.[37] The BLA estimated from the optimized geometry is defined as the difference of averaged single-bond length and averaged double-bond length on the backbone. For **PEDOP-M**, the averaged single-bond length and averaged double-bond length on the backbone are 1.421 and 1.393 Å, respectively, and thus the corresponding BLA is 0.028 Å. On the other hand, the averaged single-bond length, averaged double-bond length, and BLA of **PEDOP** are 1.426, 1.393, and 0.033 Å, respectively. It suggests that the incorporation of the methine bridge to **PEDOP** results in the smaller BLA of **PEDOP-M**.

The estimated band gap for **PEDOP-M** is 0.68 eV, which is much smaller than that of **PEDOP** with 2.44 eV. The band gap reduction is probably attributed to the smaller bond length alternation of **PEDOP-M** than the **PEDOP**, as described above. If the bond length alternation is small, the HOCO (highest occupied crystal orbital) antibonding interaction would be strengthened but the bonding interaction would be weakened. However, the case of LUCO (lowest unoccupied crystal orbital) shows a reverse trend as that of the HOCO: the bonding interaction would be strengthened whereas antibonding interaction would be weakened.[38] In this case, the HOCO level of the **PEDOP-M** is destabilized by 0.44 eV, and the LUCO level of the **PEDOP-M** is stabilized by 1.32 eV relative to those of **PEDOP**. The above variation on the band structure results in much smaller band gap of **PEDOP-M** as compared to **PEDOP**. The smaller IP of **PEDOP-M** also indicates the lower oxidation potential of **PEDOP-M** as compared to **PEDOP**. The theoretical results suggest that the methine-bridged **PEDOP-M** has a much smaller band gap than parent **PEDOP**.

Another interesting issue is to compare the difference on the theoretical electronic structures of methine bridged **PEDOP** and polypyrrole. The theoretical electronic properties of the methine bridged pyrrole using the same methodology are described as below: IP (3.20 eV), EA (2.47 eV), and Eg (0.73 eV). In comparison, the electronic properties of **PEDOP-M** are IP (2.54 eV), EA (1.86 eV), and Eg (0.68 eV). The incorporation of the dioxy group leads to the lower IP of methine bridged **PEDOP** than that of the methine bridged pyrrole.

Polymer Synthesis and Structure

The solubility of **PEDOP-M** would be poor for characterization and thus **PbEDOP-b** (**3a**) and **PbEDOP-nb** (**3b**) with a bulky side group were synthesized for exploring the electronic properties. Similar to the reported **PTM**,[15,16] the polymer products obtained from the acid-catalyzed polymerization of the **bEDOP** with aldehydes were highly colored, indicating its conjugated backbone. The obtained polymers were soluble in

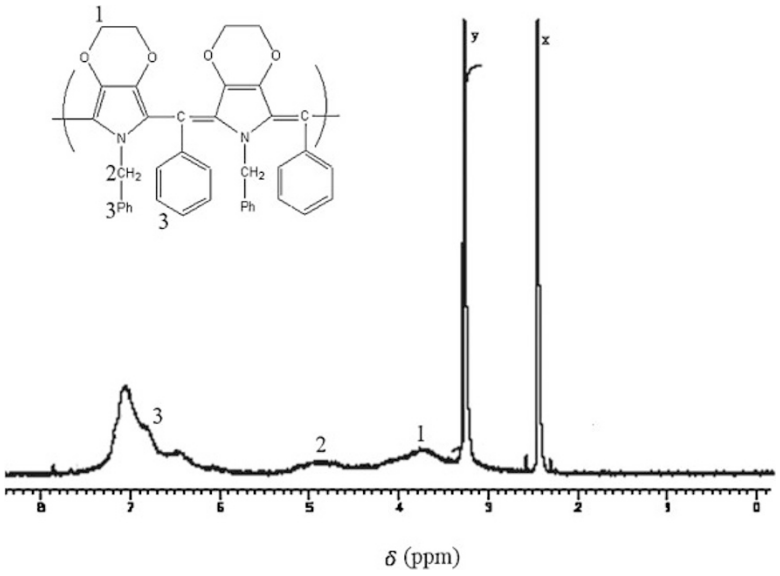

Figure 2. The ^{1}H NMR spectra of the **PbEDOP-b** in dimethyl sulfoxide-d_6 (DMSO). The peaks labeled as x and y are assigned to the DMSO solvent and water, respectively.

organic solvents, such as $CHCl_3$, DMF, DMSO, acetone, and THF, at room temperature. The average molecular weights (M_w, PDI) measured by GPC with respect to PS standard of **PbEDOP-b** and **PbEDOP-nb** are (4930, 1.62) and (5160, 1.30), respectively.

Figure 2 illustrates the ^{1}H NMR spectrum of **PbEDOP-b** in DMSO-d_6. The peaks labeled as x and y are assigned to the DMSO solvent ($\delta = 2.5$ ppm) and water in DMSO-d_6 ($\delta =$ 3.3 ppm), respectively. The broad proton resonance around 3.73 ppm is attributed to be the ethylenedioxy moiety of **PbEDOP-b**. Note that the same proton resonance of **PbEDOP-nb** is around 3.93 ppm as shown in the supporting information (Figure S1). The absence of proton signal in the region of 5.5–6.0 ppm suggests that **PbEDOP-b** is fully dehydrogenated. **PbEDOP-nb** also shows the fully dehydrogenated NMR spectrum. The electron-donating ethylenedioxy moiety could enhance dehydrogenation reactivity and facilitate the formation of the quinoid moieties, which leads to the desired conjugated polymers. Figure 3 shows the FT-IR absorption spectra of the **PbEDOP-b** and **PbEDOP-nb** in the range of 500–4000 cm^{-1}. The absorption band at 2850–3000 cm^{-1} is contributed from the C-H stretching vibration of methylene group on the ethylenedioxy-ring or benzyl group. The absorption band at 3100 cm^{-1} represents the C-H stretching vibration (-sp^2) of pyrrole or phenyl rings. The absorption peaks within 1600–1700 cm^{-1} suggest that the formation of the quinoid geometry in the main chain. The C=C double bond in the main chain rings shows its symmetric and asymmetric absorption at 1450 and 1500 cm^{-1}, respectively. The two strong absorption bands at 1343 and 1516 cm^{-1} in the spectrum of **PbEDOP-nb** are assigned to the symmetric and asymmetric of stretching vibration of N-O and N=O bonding in the *p*-nitrobenzylidene moiety, respectively. The rather weak bands at 2869 cm^{-1} in **PbEDOP-nb** are probably attributed to the overtones of the NO_2 symmetric stretching vibration bands. The absorption band at 1250 cm^{-1} of **PbEDOP-b** and **PbEDOP-nb** are assigned to the C-O-C stretching vibrations from the ethylenedioxy moiety. The NMR and FT-IR results agree well with the proposed structures of polymer **3** shown in Scheme 1.

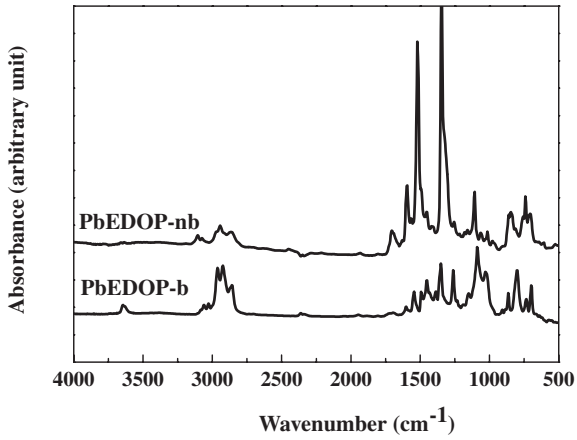

Figure 3. FT-IR absorption spectra of the **PbEDOP-nb** and **PbEDOP-b** on KBr in the range of 500–4000 cm^{-1}.

The elemental analysis results of these two polymers show a fair agreement with theoretical compositions. The analytic data of these two polymers showed about 2% difference with the expected carbon content, which are probably due to the end group effect of low molecular weight polymers.

Thermal Properties

Figure 4 shows the TGA curves of **PbEDOP-b** and **PbEDOP-nb** under nitrogen atmosphere. The thermal decomposition temperatures of **PbEDOP-b** and **PbEDOP-nb** are 300 and 281 °C, respectively. The slight weight loss at the early stage of heating is probably resulting from the easy disruption

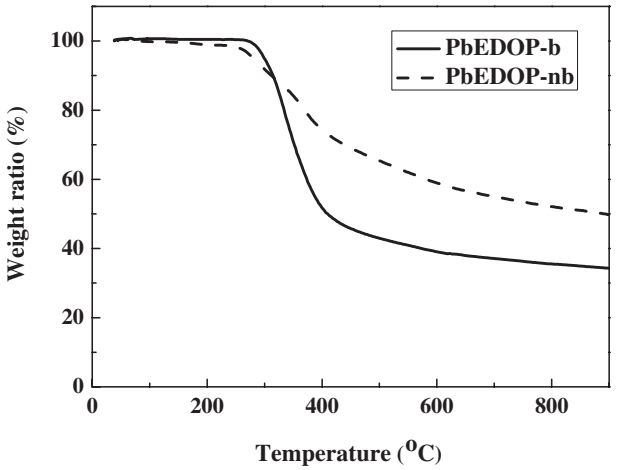

Figure 4. TGA curves of the **PbEDOP-nb** and **PbEDOP-b** obtained in flowing N_2 at a heating rate of 20 °C/min.

of the ethylenedioxy moieties. No observable glass transition temperature (T_g) is observed in the DSC curves, indicating rigid backbones of methine-bridged **PbEDOPs**.

Optical and Electrochemical Properties

Figure 5 shows the UV–vis–NIR absorption spectra of the **PEDOP-nb** and **PEDOP-b** solution in THF and thin films, respectively. In Figure 5(a), the absorption maxima (λ_{max}) of **PbEDOP-nb** in THF are observed at 240, 266, 388, and 589 nm, respectively. The absorption bands with the λ_{max} at 240 and 266 nm is assigned to the π-π^* transition of the ethylenedioxypyrrole and *p*-nitrobenzylidene moieties, respectively. The other two absorption peaks at 388 and 589 nm in **PbEDOP-nb** are attributed to highly conjugated moieties with different degree of conjugation. The absorption spectrum of **PbEDOP-b** in THF shows two major absorption bands at 237 and 516 nm, which are attributed to the EDOP and π-conjugated backbone, respectively. The larger λ_{max} of **PbEDOP-nb** than that of **PbEDOP-b** is attributed to the extended π–electron delocalization from the nitrobenzene group on the side chain. Another possibility is donor-aceptor intramolecular charge transfer between EDOP and nitrobenzene moieties. The absorption spectrum of **PbEDOP-nb** film shows three major absorption bands with λ_{max} at 269, 395, and 623 nm, respectively. Similarly, for the **PbEDOP-b** film, two major absorption bands at 204 and 522 nm are observed and that at 522 nm is attributed to highly π-conjugated backbone. The film absorption spectra of both polymers are red-shifted from that of solution due to the enhanced interchain interaction. The estimated band gaps of the **PbEDOP-nb** and **PbEDOP-b** from the absorption edges are about 1.45 and 1.77 eV, respectively. They are significantly smaller than those (2.0–3.4 eV) of **PXDOPs**.[30] It suggests the successful reduction of band gap through the incorporation of methine bridge.

The electronic structure and properties of the **PbEDOP-b** were further explored by cyclic voltammetry. Figure 6 shows the cyclic voltammogram (CV) of the **PbEDOP-b** in the potential range from −2 to 1 V (*vs.* SCE) at the sweep rate of

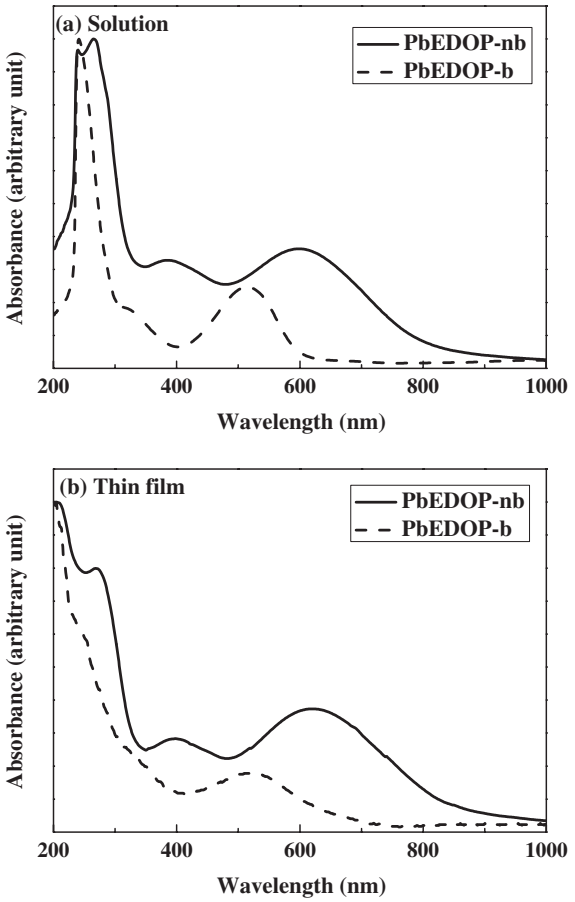

Figure 5. The UV-vis-NIR absorption spectra of **PbEDOP-nb** and **PbEDOP-b** in THF (a), and in thin films (b).

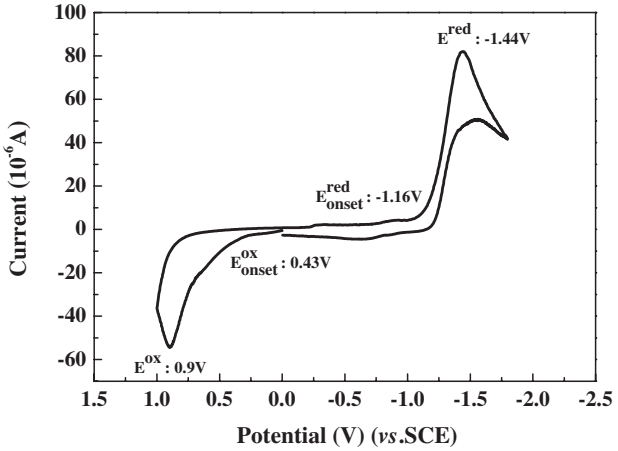

Figure 6. Cyclic voltammogram of the **PbEDOP-b** in 0.1 M $TBABF_4$/acetonitrile solution at a sweep rate of 40 mV/s.

40 mV/s. The peak potentials (E_p) for the electrochemical oxidation and reduction of the **PbEDOP-b** are shown at +0.90 and −1.44 V, respectively. The onset potentials (E_{on}) for the oxidation and reduction of **PbEDOP-b** are shown at +0.43 and −1.16 V, respectively, which correspond to an ionization potential (IP) of 4.89 eV and electron affinity of 3.30 eV,

respectively. Thus, the electrochemical band gap (E_g^{el} = IP − EA) of the **PbEDOP-b** is estimated to be 1.59 eV, which is lower than the optical band gap of 0.18 eV. **PbEDOP-nb** is very soluble in most solvents for CV measurement and its electrochemical properties could not be obtained, including acetonitrile, propylene carbonate, dichloromethane, and benzonitrile. Nevertheless, the electrochemical properties confirm that the band gap of the methine-bridged **PbEDOP-b** is smaller than that of **PEDOP** around 2.0 eV, which is in consistent with the theoretical results.

CONCLUSIONS

New small band gap conjugated polymers of methine bridged conjugated poly(3,4-ethylenedioxypyrrole) were studied. The theoretical analysis suggested that the incorporating methine-bridge into poly(3,4-ethylenedioxypyrrole) decreased the bond length alternation and led to the reduction of band gap. The theoretical band gap of **PEDOP-M** was 0.68 eV, significantly smaller than that of **PEDOP** with 2.44 eV. Two soluble methine-bridged poly(3,4-ethylenedioxypyrrole), **PbEDOP-b** and **PbEDOP-nb**, were successfully synthesized by acid-catalyzed polymerization. The experimental band gaps of **PbEDOP-b** and **PbEDOP-nb** also suggested the small band gap characteristics. The small band gap characteristics of new methine-bridged poly(3,4-ethylenedioxypyrrole) may have potential applications in electronic and optoelectronic applications.

Acknowledgment. The financial supports from National Science Council, the Ministry of Education, and the Ministry of Economic Affairs of Taiwan are highly appreciated.

Electronic Supporting Information Available: Figures S1. These materials are available *via* the Internet at http://www.spsj.or.jp/c5/pj/pj.htm

Received: October 18, 2008
Accepted: January 13, 2009
Published: March 4, 2009

REFERENCES

1. J. Roncali, *Chem. Rev.*, **97**, 173 (1997).
2. H. A. M. van Mullekom, J. A. J. M. Vekemans, E. E. Havinga, and E. W. Meijer, *Mater. Sci. Eng., R*, **32**, 1 (2001).
3. N. Matsumi and Y. Chujo, *Polym. J.*, **40**, 77 (2008).
4. E. Bundgaard and F. C. Krebs, *Sol. Energy Mater. Sol. Cells*, **91**, 954 (2007).
5. F. Zhang, W. Mammo, L. M. Andersson, S. Admassie, M. R. Andersson, and O. Inganäs, *Adv. Mater.*, **18**, 2169 (2006).
6. C. Soci, I.-W. Hwang, D. Moses, Z. Zhu, D. Waller, R. Gaudiana, C. J. Brabec, and A. J. Heeger, *Adv. Funct. Mater.*, **17**, 632 (2007).
7. W. Y. Lee, C. W. Chen, C. C. Chueh, C. C. Yang, and W. C. Chen, *Polym. J.*, **40**, 249 (2008).
8. W. C. Wu, W. Y. Lee, and W. C. Chen, *Macromol. Chem. Phys.*, **207**, 1131 (2006).
9. A. P. Kulkarni, Y. Zhu, and S. A. Jenekhe, *Macromolecules*, **38**, 1553 (2005).
10. Y. Lee, S. Sadki, B. Tsuie, and J. R. Reynolds, *Chem. Mater.*, **13**, 2234 (2001).
11. F. Fusalba, H. A. Ho, L. Breau, and D. Belanger, *Chem. Mater.*, **12**, 2581 (2000).
12. R. Kiebooms, I. Hoogmartens, P. Adriaensens, D. Vanderzande, and J. Gelan, *Macromolecules*, **28**, 4961 (1995).
13. H. Meng and F. Wudl, *Macromolecules*, **34**, 1810 (2001).
14. S. A. Jenekhe, *Nature*, **322**, 345 (1986).
15. W. C. Chen and S. A. Jenekhe, *Macromolecules*, **28**, 465 (1995).
16. M. Hanack, U. Schmid, S. Echinger, F. Teichert, and J. Hieber, *Synthesis*, 634 (1993).
17. Q. Zhang, M. Yang, P. Wu, and H. Ye, X. Liu, *Synth. Met.*, **156**, 135 (2006).
18. M. Karikomi, C. Kitamura, S. Tanaka, and Y. Yamashita, *J. Am. Chem. Soc.*, **117**, 6791 (1995).
19. J. Kastnar, H. Kuzamany, D. Vegh, M. Landl, L. Cuff, and M. Kertesz, *Macromolecules*, **28**, 2922 (1995).
20. T. L. Lambert and J. P. Ferraris, *J. Chem. Soc., Chem. Commun.*, **11**, 752 (1991).
21. C. Quattrocchi, R. Lazzaroni, J. L. Bredas, R. Zamboni, and C. Taliani, *Macromolecules*, **26**, 1260 (1993).
22. C. J. Neef, I. D. Brotherston, and J. P. Ferraris, *Chem. Mater.*, **11**, 1957 (1999).
23. R. Kiebooms and F. Wudl, *Synth. Met.*, **101**, 40 (1999).
24. R. H. L. Kiebooms, H. Goto, and K. Akagi, *Macromolecules*, **34**, 7989 (2001).
25. H. Goto and K. Akagi, *J. Polym. Sci., Part A: Polym. Chem.*, **43**, 616 (2005).
26. T. Benincori, S. Rizzo, F. Sannicolò, G. Schiavon, S. Zecchin, and G. Zotti, *Macromolecules*, **36**, 5114 (2003).
27. W. C. Chen, C. L. Liu, C. T. Yen, F. C. Tsai, C. J. Tonzola, N. Olson, and S. A. Jenekhe, *Macromolecules*, **37**, 5959 (2004).
28. M. B. Zaman and D. F. Perepichka, *Chem. Commun.*, 4187 (2005).
29. P. Schottland, K. Zong, C. L. Gaupp, B. C. Thompson, C. A. Thomas, I. Giurgiu, R. Hickman, K. A. Abboud, and J. R. Reynolds, *Macromolecules*, **33**, 7051 (2000).
30. G. Sonmez, P. Schottland, K. Zong, and J. R. Reynolds, *J. Mater. Chem.*, **11**, 289 (2001).
31. R. M. Walczak and J. R. Reynolds, *Adv. Mater.*, **18**, 1121 (2006).
32. K. Zong and J. R. Reynolds, *J. Org. Chem.*, **66**, 6873 (2001).
33. Gaussian 03, Revision B.4, M. J. Frisch, G. W. Trucks, H. B. Schlegel, G. E. Scuseria, M. A. Robb, J. R. Cheeseman, J. A. Montgomery, T. Vreven, Jr., K. N. Kudin, J. C. Burant, J. M. Millam, S. S. Iyengar, J. Tomasi, V. Barone, B. Mennucci, M. Cossi, G. Scalmani, N. Rega, G. A. Petersson, H. Nakatsuji, M. Hada, M. Ehara, K. Toyota, R. Fukuda, J. Hasegawa, M. Ishida, T. Nakajima, Y. Honda, O. Kitao, H. Nakai, M. Klene, X. Li, J. E. Knox, H. P. Hratchian, J. B. Cross, C. Adamo, J. Jaramillo, R. Gomperts, R. E. Stratmann, O. Yazyev, A. J. Austin, R. Cammi, C. Pomelli, J. W. Ochterski, P. Y. Ayala, K. Morokuma, G. A. Voth, P. Salvador, J. J. Dannenberg, V. G. Zakrzewski, S. Dapprich, A. D. Daniels, M. C. Strain, O. Farkas, D. K. Malick, A. D. Rabuck, K. Raghavachari, J. B. Foresman, J. V. Ortiz, Q. Cui, A. G. Baboul, S. Clifford, J. Cioslowski, B. B. Stefanov, G. Liu, A. Liashenko, P. Piskorz, I. Komaromi, R. L. Martin, D. J. Fox, T. Keith, M. A. Al-Laham, C. Y. Peng, A. Nanayakkara, M. Challacombe, P. M. W. Gill, B. Johnson, W. Chen, M. W. Wong, C. Gonzalez, and J. A. Pople, Gaussian, Inc., Pittsburgh P.A., 2003.
34. A. D. Becke, *J. Chem. Phys.*, **98**, 5648 (1993).
35. C. Lee, W. Yang, and R. G. Parr, *Phys. Rev. B*: Condens. Matter Mater. Phys., **37**, 785 (1988).
36. B. Miehlich, A. Savin, H. Stoll, and H. Preuss, *Chem. Phys. Lett.*, **157**, 200 (1989).
37. Y. S. Lee and M. Kertesz., *J. Chem. Phys.*, **88**, 2609 (1988).
38. R. Hoffmann, C. Janiak, and C. Kollmar, *Macromolecules*, **24**, 3725 (1991).